Egyptian Journal of Geology

https://egjg.journals.ekb.eg

Application of Enhanced Techniques of Aeromagnetic Data to Study Subsurface Structure in El-Urf Area, Northern Eastern Desert, Egypt

Noha M.F. Hassan[1], Mostafa A. M. Zaeimah*[2], Mohamed F. Abu-Hashish[1] and **Manar M. Elborm[1]**

Geology Department, Faculty of Science, Monufia University, Monufia, Egypt

Exploration Division Head of the Department of Geophysical follow -up of Exploration Nuclear Materials Authority

AIRBORNE magnetic data were acquired by Aero-Service, in 1984 in Egypt`s Eastern Desert, covering Gabal El-Urf area and its surroundings. Precambrian basement rocks (PBR) are dominated by younger granites (Gy). Furthermore, region of study may contain radioactive materials. The magnetic measurements indicate variations in the sources' depths and magnetic susceptibilities. Therefore, this data is used to find out the positions and depths of the magnetic bodies they have formed. This work deals with separation of RTP map to detect the regional (deep seated) and the Residual (shallow seated) magnetic bodies by using radially averaged power spectrum. Usage of separation illustrated that, the igneous basement components within range depths from 200m to more than 1500m and less than 200m for noise component. By Using Source Parameter imaging technique, this depth method shows comparable outcomes. The basement sources are located between 150 to about 1500 meters below the surface. The structural frameworks of the area and basement faults have been identified through investigation and interpretation of magnetic data. NE-SW is the major fault trend for RTP map from rose diagram in the study region. There are also other trends North West – South East and East -West. For Regional map, the major trend of the study area is North North East (NNE) –South South West (SSW). Additionally, there are other trends NW-SE and NE-SW. For Residual map the major trends of the research region are NW-SE, NE-SW, WNW-ESE and E-W. This work detects the suggested Faults along two W-E Profiles and another two perpendicular S-N Profiles and detects the depth values of their intersection point. The valleys' depth in the research area is the final and most significant finding in relation to the study's goal. This is because radioactive materials are thought to be trapped by it.

Keywords: Reduction to the North Magnetic Poles, Basement Surface, Source Parameter Image, Horizontal Derivatives, Tilt Derivatives, Analytic Signals, Northern Eastern Desert.

1. Introduction

Gabal El-Urf area and its surroundings, which cover around 340 km^2, represent an exposure of Neoproterozoic basement in Egyptian Eastern Desert. This region is mainly composed of massive granitic masses. Its length is around 14 km, and its width varies from 600 m to over 2 km. According to Asran et al. (2013), it is visible like an extended (elongated) mass that spreads out in the NNE-SSW direction.

This study area is situated in Egyptian northern region of the Eastern Desert **(Figure 1)**. It lies between latitudes 26°36/ and 26°44/ N and longitudes 33°18/ and 33°32/ E. The region has a high terrain, associated with the presence of high mountains.

Magnetic prospecting looks for changes in the earth`s magnetic field that resulted from changes in the underlying geological structure or by variations in the magnetic characteristics of near –surface rocks.

Magnetic susceptibility refers to rocks' inherent magnetism. Strong positive anomalies are related to basic and ultrabasic rocks, whereas acidic rocks are related to strong negative anomalies.

2. Geologic Setting

According to Stern (1994) and Kusky (2003), The Pan-African Arabian Nubian shield, extending from Ethiopia and Uganda in the south to Egypt in the north, includes the basement complex that formed in Egypt's Eastern Desert (EED).

*Corresponding author e-mail: mostafazaaeima@yahoo.com
Received: 15/09/2024; Accepted: 28/09/2024
DOI: 10.21608/EGJG.2024.319605.1091

EED was separated into three different basement domains by two fault zones that form its geological background: the North Eastern Desert (NED), the Central Eastern Desert (CED), and the Southern Eastern Desert (SED). NED and SED have higher concentrations of granitic rocks than CED, (Hamimi, Z et al., 2022 and 2023).

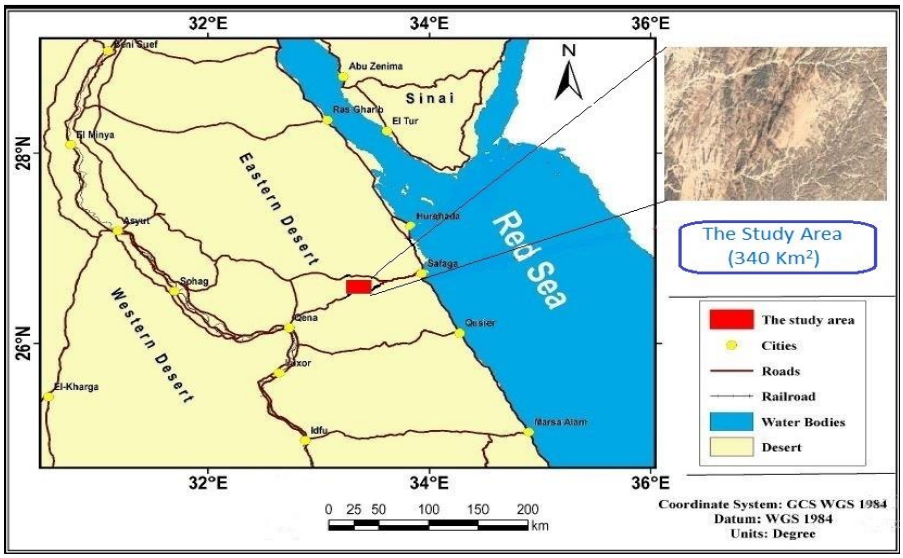

Fig. 1. Location map of Gabal El-Urf area, North Eastern Desert, Egypt.

Massive masses of granite porphyry and quartz diorites, intruded by basic dykes, quartz veins, moreover, pegmatite pockets, compose the majority of the study area. Dry Wadis, or dry valleys, cut through these rocks and are filled by Quaternary sediments (El-Tahir, 1978).

Quaternary sediments and Precambrian basement rocks mostly dominate this region. According to their field relationships and observations, the exposed rock units in the El-Urf region **(Figure 2)** have been divided chronologically into the following categories (El-Tahir, 1978):

(5) Pegmatite and post granitic dykes……. (Youngest)

(4) Younger granites — Synogranites; Monzogranites

(3) Younger gabbro

(2) Older granites

(1) Metavolcanics ……..... (Oldest)

Metavolcanic rocks are the oldest kind of rocks in the El-Urf region. They are located in its south western part and appear in belts extending from NE to SW direction. Older granites usually show monumental shapes, cavernous weathering, medium-to coarse-grains, differing in color from white to dark grey. It also usually exhibits low to moderate relief and are located in the eastern and southern regions of the study area.

Younger gabbro is in almost all of the study area's central regions, as small, rounded and/or elongated bodies that arise in mild to moderate relief. Massive monzogranites in El-Urf are clearly identified from the surrounding rocks by their distinctive pink and/or red color. These rocks are visible in the northern and western parts of the study region.

Synogranites with high to moderate relief are the predominant younger granite rock type in the research region. Synogranite varies in medium to coarse grain sizes.

Pegmatites and post-granite dykes have granitic compositions and coarse to very coarse grains. They can be divided into zoned and unzoned pockets. In G. El-Urf, zoned pockets dominate as subrounded pockets of relatively small size (El-Mansi and Dardier, 2005). G. Abu Shihat granites, which are situated in the middle region of the research area, are dominated by unzoned pockets. The pegmatitic body, known as Wadi Abu-Shihat, is located southwest of Gabal El-Urf. The other pegmatite body known as Abu Zawal is located northeast of Gabal El-Urf (Asran et al., 2013).

3. Structural Setting

The Eastern Egyptian Desert's basement belt has a very complicated structure. From landsat images, hundreds of lineaments were mapped, the majority of these can be correlated with faults, shear zones, dykes, and folds that are well-known. The faults within the research region show many trends. The main trends

that they follow are NE-SW and NNE-SSW. They are longer than the other trends (ENE-WSW, NNW-SSE, NW-SE, N-S and E-W) as shown in **(Figure 3).**

The measured faults vary in length from 1.8 km to 26.36 km and in width from less than one meter to 500 meters.

Two major sets of trends in the research region that are observed: the first trend has the majority of faults and generally trending in a NNE-SSW direction, the other is taking the North East-South West. Less common fault sets, ENE-WSW, NW-SE, and N-S, are grouped in decreasing order of occurrence (Abd-El Ghani, 2001). The most common type is represented by dyke swarms that extend southward along Wadi Fatirah El-Beidah and strike in a NNE-SSW direction. The NE-SW trend of these dykes corresponding with Wadi Abu-Zawal. Their dips range from nearly vertical to nearly horizontal, and their thicknesses range from less than one meter to more than five meters. The dykes have a felsic-mafic composition. According to Abd-El Ghani (2001), these dykes cut through all of the different rock groups. Including the felsic units, which exhibit high relief and the intermediate and mafic levels displaying low relief.

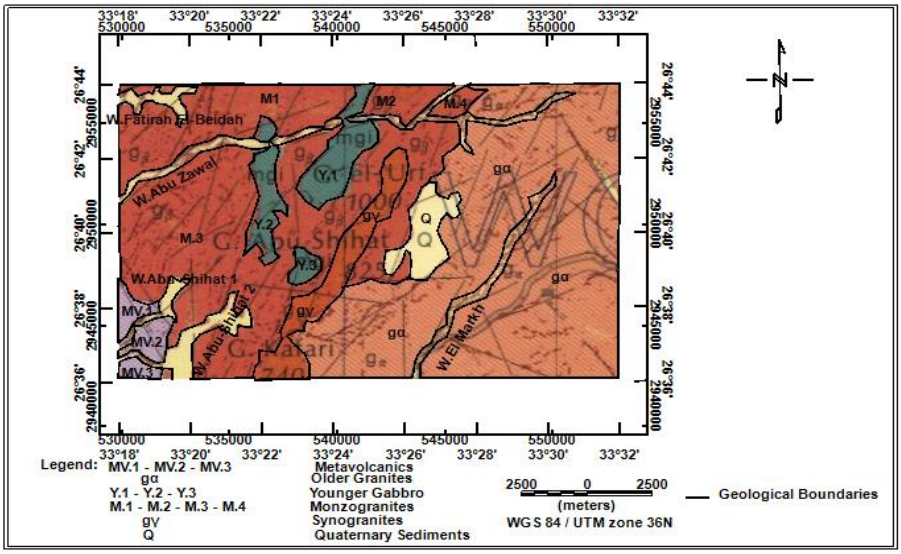

Fig. 2. Geologic map of Egypt's Northern Eastern Desert, Gabal El-Urf region (Conoco, 1987).

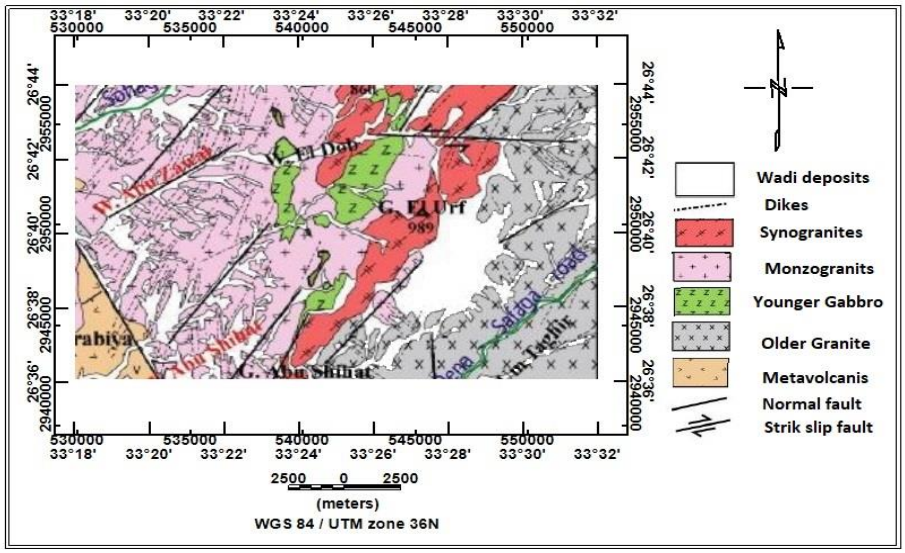

Fig. 3. Structure map of Egypt's Northern Eastern Desert, Gabal El-Urf region, (Abu El-Leil et al., 2015).

4. Data Acquisition and Methods

The majority of Egypt's Eastern Desert and a small portion of its Central Western Desert were subjected to an aerial gamma-ray spectrometry and geomagnetic survey in 1982. It was as a part of the Egyptian General Petroleum Corporation (EGPC), the MPGAP project, which was cooperation between the Egyptian Geological Survey and Mining Authority (EGMA), and the Aero-Service Division of the Western

Geophysical Company of America, USA. The purpose of the survey was to acquire data to help identify and evaluate the region's groundwater, mineral and petroleum resources. The flight lines had an azimuth of 45 and 225 degrees and an orientation of NE-SW.

The distance between the flying lines was over 1.5 kilometres. The tie lines had 10 km flight line spacing and were aligned NW-SE at 135^{o} and 315^{o} azimuth. The aircraft had a nominal flying elevation of 120 meters above the ground, and its average ground speed varied between 222 and 314 km/h (Aero-service, 1984). Oasis montaj version 8.3.4 was utilized in the magnetic data processing derived from the Reduction to the Poles (RTP) map using several techniques (Geosoft program, 2015).

5. Geophysical Data Processing

The fundamental principle of the geomagnetic tool approach is the detection of minute variations in the magnetic field, which might be due to topographic relief, structural relief, or inhomogeneity in the composition of the basement rocks. These changes can be measured on the ground or, more frequently, with the use of appropriate instruments carried by an aircraft. Therefore, the targets of geomagnetic survey are to identify shape, depth, position, and attitude of the responsible magnetic bodies within a given area. These values are then to be interpreted using geological models that are consistent with both the observed geology and accepted geological theory (Boyd, 1969).

The reduction of the total intensity aeromagnetic map (TOT) to an RTP map was done in order to minimize variations in the earth's magnetic field. Baranov, 1957; Baranov and Naudy, 1964; Bhattacharyya, 1965 and 1967; and Baranov, 1975 are the first to describe the Reduced to the Pole approach.

6. Results

6.1. Reduction to the northern magnetic pole (RTP) map

The RTP map **(Figure 4)** displays variety of anomalies with variable frequencies and amplitudes that reflect their various sources, depths, and compositions.

6.2. Magnetic Separation

The primary goal of the magnetic separation used in this study is to separate the residual magnetic anomalies caused by the shallow-seated sources from the regional magnetic anomalies produced by the deep-seated sources. The Reduction to the Pole map is separated to distinguish between structures of a local and regional nature.

6.2.1. Radially averaged power spectrum

The spectrum analysis approach is used to provide deep information about a system of anomalies or a group of bodies. It is based on the Fourier Transform analysis of the magnetic data (Spector and Grant, 1970, Garcia and Ness, 1994, and Maurizio et al. 1998). The power spectrum is obtained using the Fast Fourier Transform (FFT) on the RTP data in this study in order to estimate average depths and regional-residual separation. Based on the investigation of the two-dimensional power spectrum curve **(Figure 5)**, four linear segments have been identified and matched.

6.2.2. Regional magnetic component

Regional magnetic map **(Figure 6)** shows smooth and simple contour lines. Additionally, there has been an increase in positive magnetic values, which are indicated in red, and covers up two areas of the map. The first portion extends about northward and faces East-West. In addition, there are high magnetic anomalies in the center that are connected to the high anomalies in the north. While southern regions are subjected to low regional magnetic anomalies that are shaded green and blue, and extends from East to West. A second low magnetic anomaly penetrates the central high anomalies.

6.2.3. Residual magnetic component

Geophysicists have utilized residual maps to highlight local features that frequently disappear in the larger field features (Ammar et al., 1988). After subtracting the regional effect, the distribution of the geomagnetic field is displayed in the residual map **(Figure 7)**. It exhibits magnetic anomalies with varying polarities that appear to be positive and negative. Several magnetic belts are oriented nearly NNE-SSW, NW-SW and N-S. These features reflect the variations in anomalies, sources, depths, compositions, and structural settings.

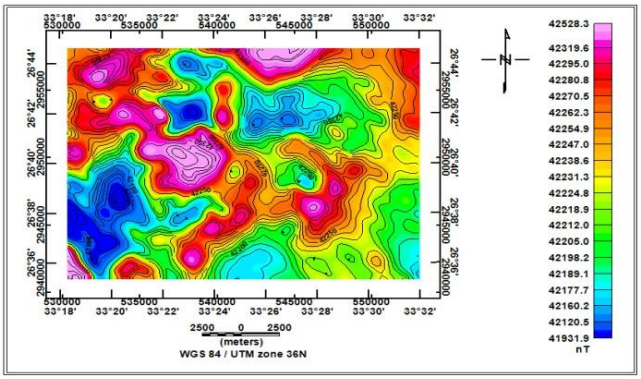

Fig. 4. Reduction to the Pole map (RTP) in El-Urf area, Northern Eastern Desert, Egypt.

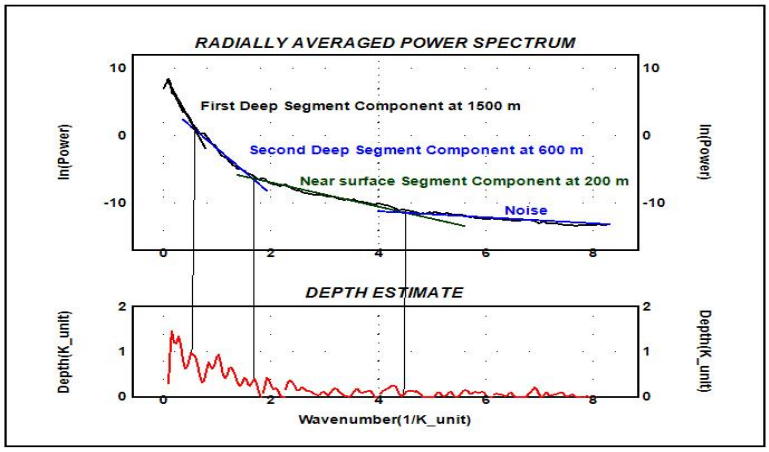

Fig. 5. RTP data's radial average power spectrum and depth estimation at El-Urf area, Egypt's Northern Eastern Desert.

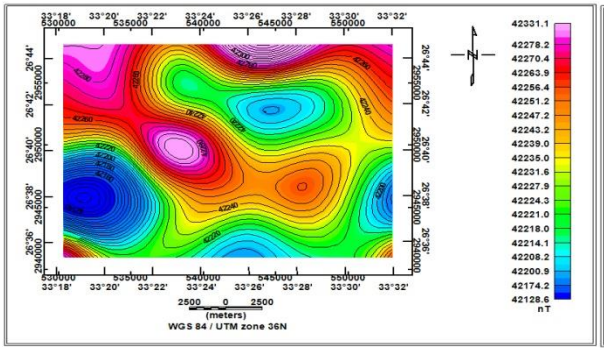

Fig. 6. Regional Magnetic map in El-Urf area, Egypt's Northern Eastern Desert.

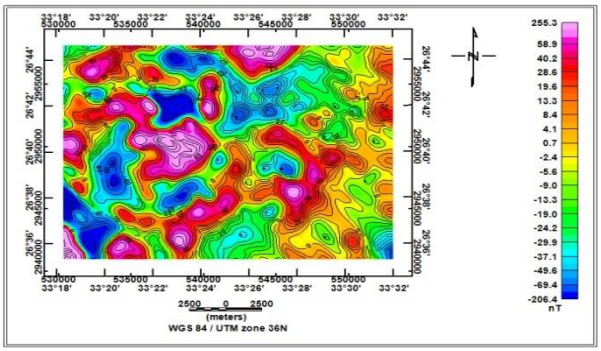

Fig. 7. Residual Magnetic map in El-Urf area, Egypt's Northern Eastern Desert.

6.3. Source Parameter Image (SPI)

Local wave number or (SPI) is a procedure (technique) for estimating magnetic depths based on the extension of complex analytical signals. This technique is available in Oasis Montaj V.8.3 (2015). This method developed after Blakely and Simpson (1986), Thurston and Smith (1997). Different colors are displayed in the SPI grid image and legend **(Figure 8)**, indicating that the magnetic susceptibility contrast varies throughout the research area. These colors might also represent the basement surface topography.

The legend's negative sign denotes a depth below the surface. According to the legend, the blue color on the map denotes regions with thick sediments, deep layers, or low magnetic anomalies. The legend's pink, purple, yellow, and orange colors represent high magnetic anomalies that are connected to the shallow basement. There are two magnetic sources, based on the depths to the magnetic sources: the shallow source and the deeper source based on the SPI results. With different sizes and trends, the magnetic source is located between 200 and 1400 meters below the surface (Crests and basins).

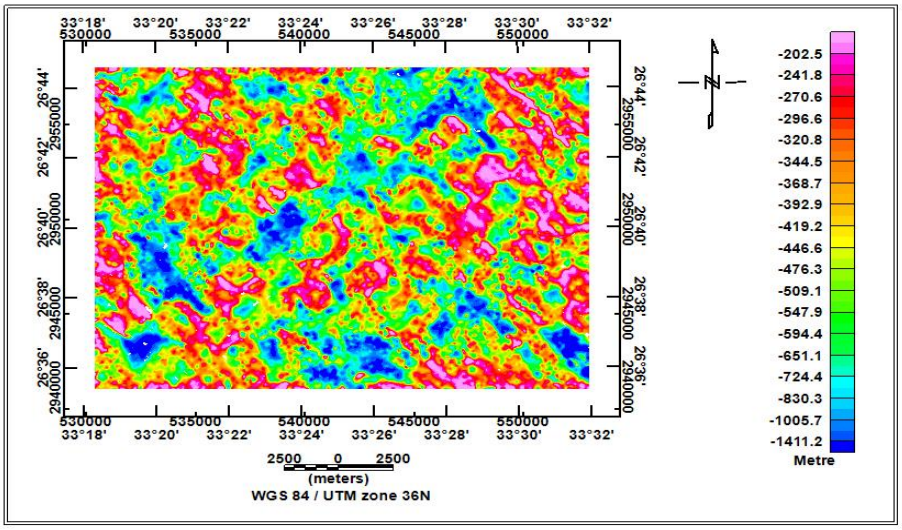

Fig. 8. Source Parameter Image (SPI) of El-Urf area, Egypt's Northern Eastern Desert

6.4. Horizontal derivatives (HDR)

According to Grauch and Johnston (2002) and Debeglia et al. (2006), (HDR) is usually employed to mark the outer boundaries of the magnetic sources and determine their orientations. The primary benefit of the horizontal gradient approach is that it is less sensitive to noise in the data because it just needs to compute the field's two first-order horizontal derivatives (Phillips, 2002). High frequency horizontal changes in the magnetic data are enhanced by the derivatives. These changes were attributed to boundaries or faults separating different geological units Verduzco et al., (2004), Lghoul et al., (2023).

In general, the horizontal gradient map **(Figure 9a)** uses the horizontal gradient approach to detect the body's borders and boundaries. High anomalies on the map, which are colored red, indicate boundaries also points of contact.

6.5. Tilt derivative (TDR) and Analytic Signal (AS)

The margins of the near-surface features have been strengthened with the application of tilt derivative (TDR) and analytic signal (AS), Verduzco et al., (2004) and Wijns et al., (2005). Tilt derivative of RTP magnetic data of the study area was calculated. Tracing susceptibility contacts may be done using the tilt derivative's zero contour. North West-South East and North East-South West fault trends predominate in the research area **(Figure 9c)**. TDR map is comparable to the vertical derivative map.

The Analytic Signal **(Figure 9e)** defines numerous features, particularly on western side, and is essentially related to differences in the lithology changes inside the basement. These local highs are caused by increasing susceptibility contrasts or are attributed to older granites and younger gabbro rocks. In addition, boundaries along the magnetic anomalies are making the sizes and depths of the basement units more and more distinct. The area is influenced by the NW anomalous zone, according to the anomaly patterns in the analytic signal map.

6.6. Vertical derivative

This technique acts as a filter because it distinguishes in terms of depth between local-shallower anomalies and larger regional ones. The method is thought to be good for identifying edges of the anomalous bodies, emphasizing sources at shallow depths, and enhancing fault patterns. The various subsurface block units are separated by significant faults (zero lines).

The vertical derivative map **(Figure 9d)** indicates that the western region exhibits substantial NW–SE and conjugate NE–SW trend patterns in terms of structural pattern. Moreover, the northern and eastern parts are also dominated by the NW- SE directions.

6.7. Trend Analysis

The principal approach of this research is to define the tectonic and structural characteristics of the El-Urf area. It can be assumed that magnetic anomalies may be associated to certain geotectonic elements since their interpretation accurately reflects the subsurface geologic image in the studied region. Resulted structural systems are displayed as rose diagrams after statistical analysis as shown in **(Figure 10).**

The trend analysis techniques applied to the interpreted structural trends that were generated and gathered from magnetic (RTP, regional, and residual)

maps. It reveals that NW-SE, EW and North E-South W structures are predominated. The tectonic activity within the area is greatly affected by these trends. As the result of widespread intrusions by both younger and older granitoids, EW and N East-S West tendencies emerged. NW-SE Faults can be explained by the opening of the Red Sea-Gulf of Suez rift Oligocene-Miocene.

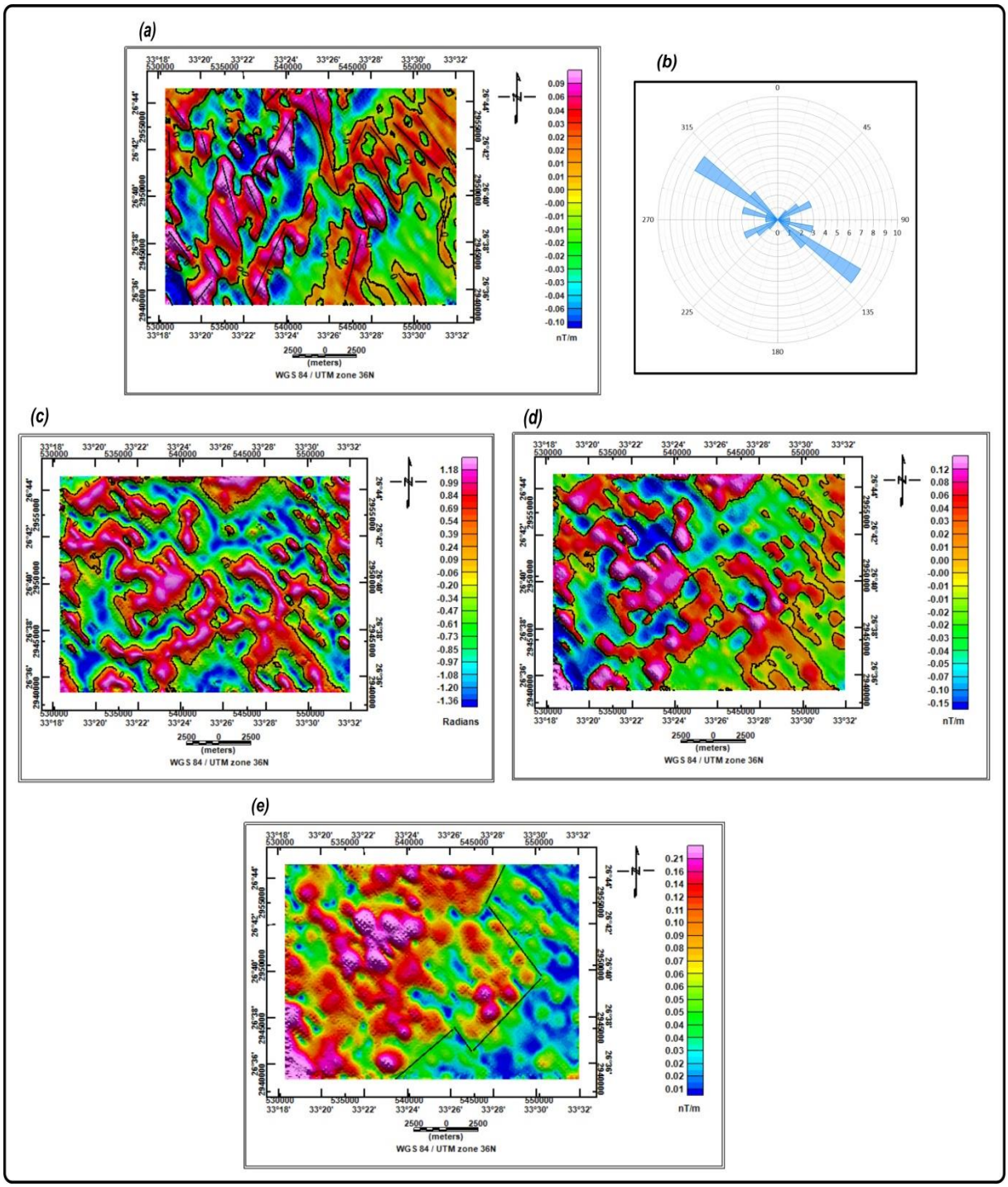

Fig. 9. (a) Magnetic field horizontal derivative (HDR), (b) Tilt derivative (TDR), (c) vertical derivative in Z, (d) Analytic Signal of the total magnetic field and (e) Rose Diagram for horizontal derivative (HDR).

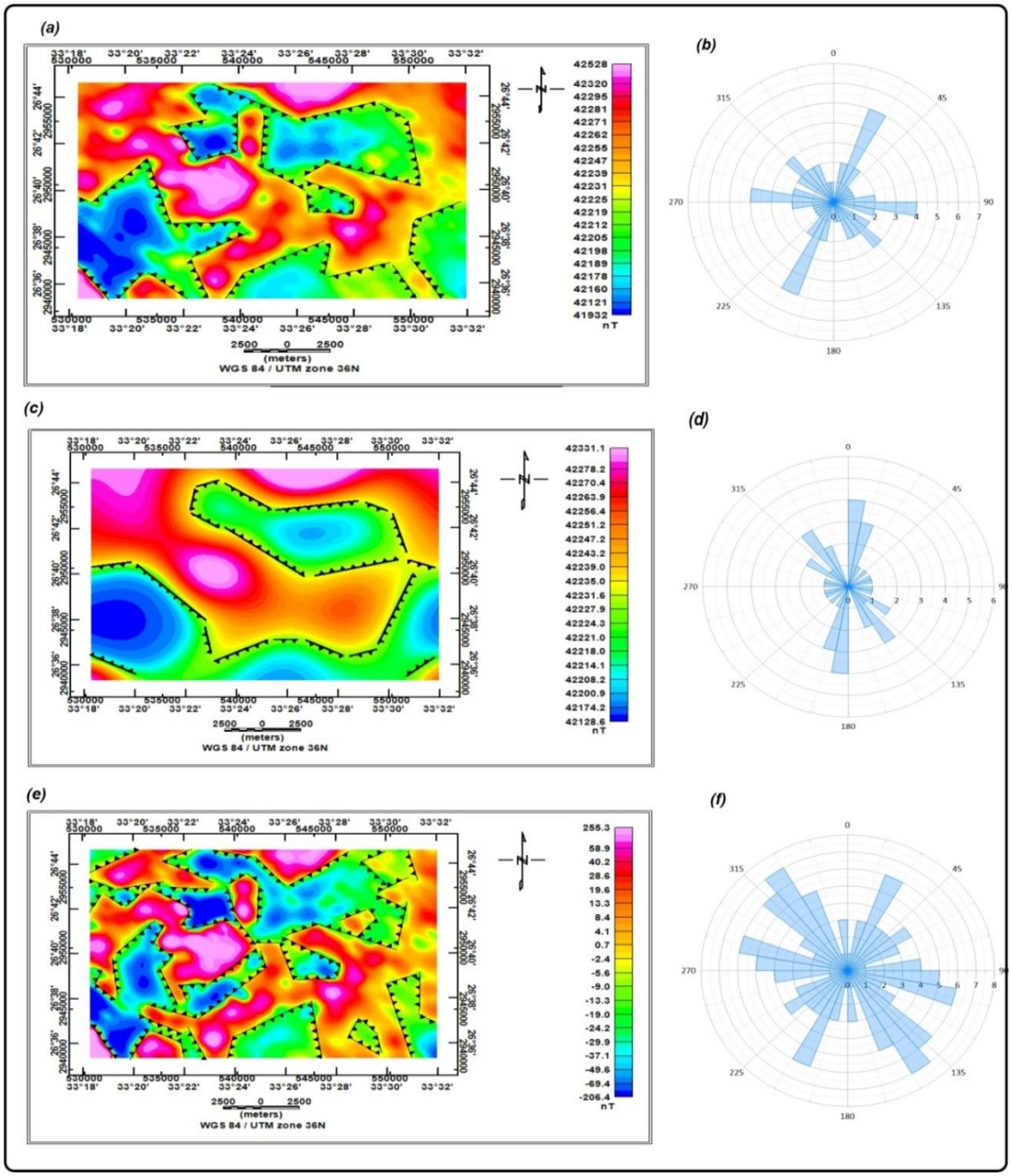

Fig. 10. Fault elements derived from (a,b) RTP map, (c,d) Regional RTP map and (e,f) Residual RTP map.

6.8. 2D magnetic modeling

2D magnetic modeling is created by GM SYS Program (2015). On the RTP magnetic map, four magnetic profiles are applied **(Figure 11)**.A pair of profiles are taken, one oriented from the West to the East and the other from the South to the North.Utilizing accessible geologic information, the previously carried out magnetic depth determinations, and the outcomes of qualitative interpretation of magnetic maps. The magnetic susceptibility contrast values have been assumed. The magnetic field is calculated iteratively for the assumed geologic model, until a good fit is reached between the observed and calculated profiles. The changes at the basement surface's (bs) topography is a result of the existence of several faults even majors or minor. These faults make uplifts at the (bs) along these profiles as follows:

The First profile P1 **(Figure 12)** has been taken along W-E direction. It is 22 Km long. The magnetic modeling for this profile indicates that the deep (bs) depth is 1.4 km at intersecting with profile P3, then the deep basement surface has been uplifted. The deep

(bs) depth along this profile becomes the shallowest at the intersection with profile P4, that reaches 400meter.

The Second profile P2 **(Figure 13)** has been taken along W-E direction. It is 23 km long. It shows different thickness values of the depth to deep (bs). This profile's magnetic modeling suggests that the deep basement surface's shallowest depth reaches to 100 m at eastern part, then the deep (bs) has been downlifted. The depth of the basement becomes the deepest at depth equal 800m, then get up to reach 400m at the intersection point with profile P4 and 230 at the intersecting with profile P3.

The Third profile P3 **(Figure 14)** has been carried out in the N-S direction. It is 17 Km long. According to magnetic model of this profile, the deep basement's shallowest depth is found at 50 m at the north western part, then the deep basement surface has been downlifted. The depth reaches to 230m with the intersection point with profile P2. The depth of the basement becomes the deepest at depth equal 1.45km, then get up to reach 1.4 Km at the intersection point at profile P1.

The Fourth profile p4 **(Figure 15)** has been taken along N-S direction. It is 18.2 km long. It shows different thickness values of the deep depth to (bs). The deep basement surface's maximum depth is reached to 450m at the Southern part of the profile with the intersection point with profile P1. Then the basement surface has been uplifted to the minimum depth equal to 200m, then down lifted at the intersecting point with profile P2 reaching to 400m depth.

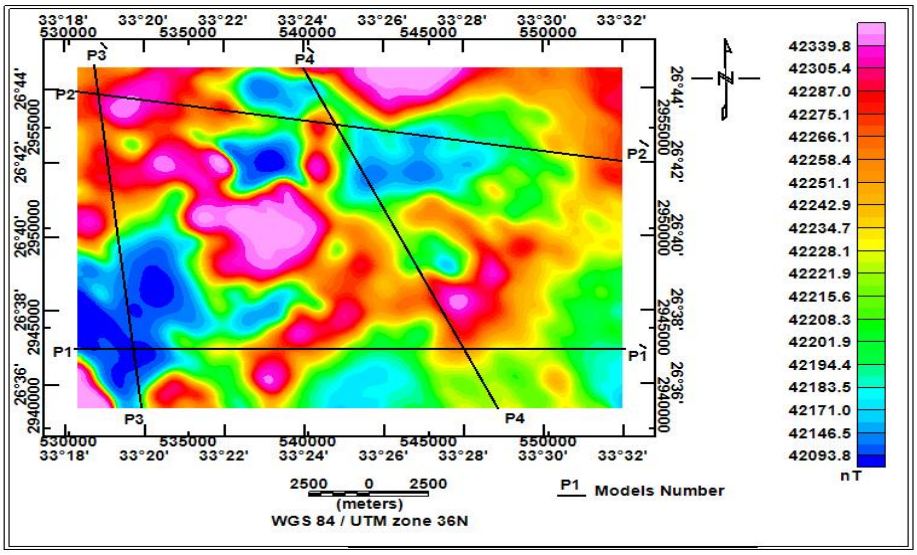

Fig. 11. 2D Models in Reduction to the Pole map (RTP) in El-Urf area, Egypt's Northern Eastern Desert.

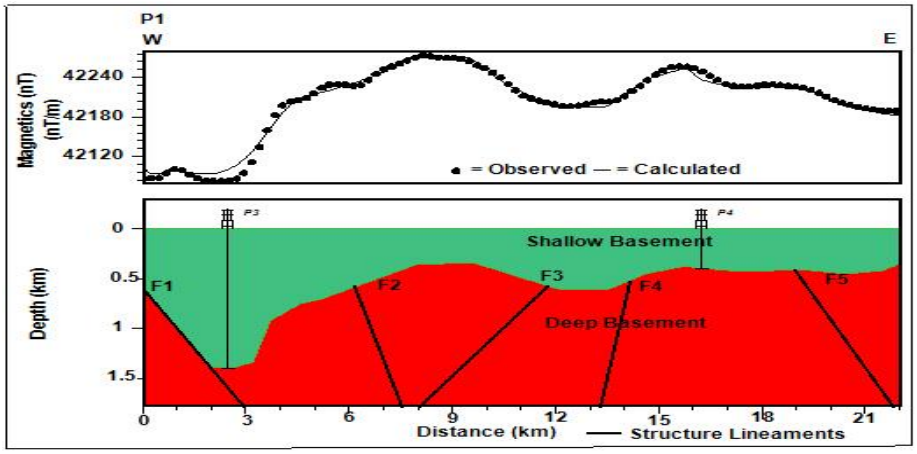

Fig. 12. 2-D model along magnetic profile P1-P1'

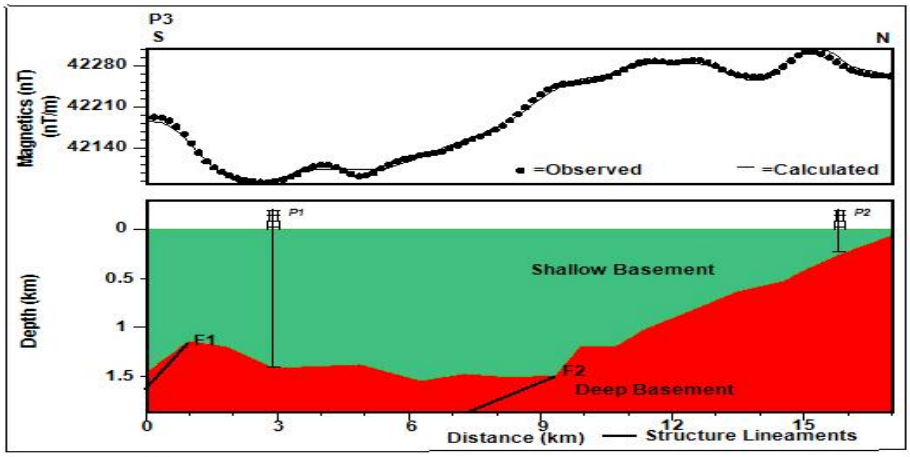

Fig. 13. 2-D model along magnetic profile P2-P2'.

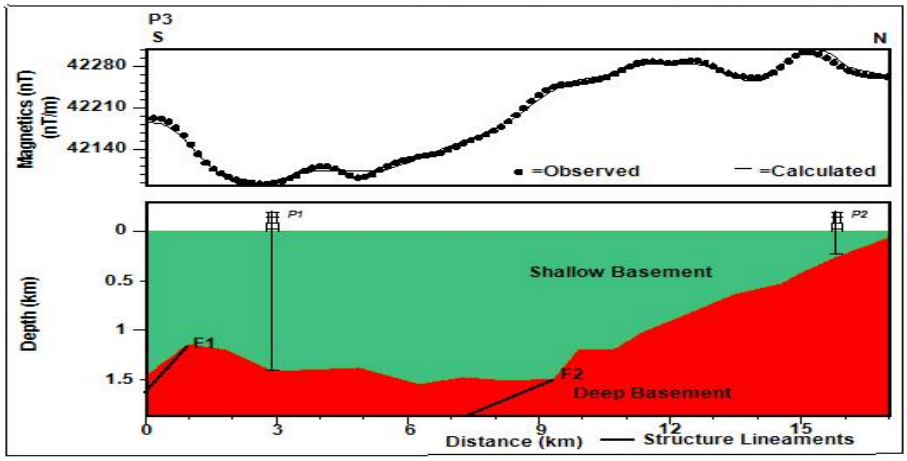

Fig. 14: 2-D model along magnetic profile P3-P3'.

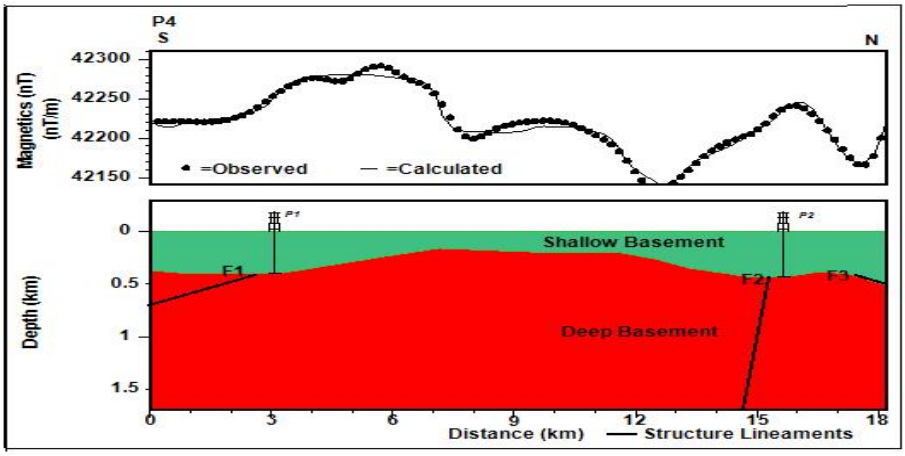

Fig. 15: 2- D model along magnetic profile P4-P4'.

7. Discussion

The Reduction to pole map in the El-Urf area, displays many anomalies with variable depths and compositions, as well as frequencies and amplitudes that reflect various sources for these anomalies. The magnetic field amplitude, which varied between 41931.9 nT and 42528.3 nT, is depicted on (RTP) map. This map shows a change in magnetic intensity that may be related to variations in basement surface lithology.

In RTP map, High anomalies have magnetic values vary from 42262 nT to 42528.3 nT. While negative anomalies with minimum ranges of magnetic values of 42189 nT, 42160 nT and 42528.3 nT. The second belt lies South latitude 26°40` N and at the same longitude as the first belt. This belt is composed of a number of high anomalies that are situated at the central part of the research area and extend to South and to South-West with maximum values of 42270 nT, 42319 nT and 42528 nT. Low anomalies exist in this belt at the South-East and South-West with minimum values of 41931 nT, 42160 nT and 42177 nT.

By using Power spectrum, Two segments divide the deep sources: the first segment wavenumbers from 0.005 to 0.75 cycles /k-unit, while the second segment lies from 0.75 and 1.8 cycles /k-unit at the regional level.While the shallow sources are characterized by wavenumbers from 1.8 to 4.33 cycles per k-unit. The spectrum's noisy region exceeds 4.33 cycles per k-unit and depth less than 200m. The estimated depths of the regional, residual and near surface sources are 1500 m, 600 m and 200 m, respectively, below the surface. From power spectrum RTP map divided into two maps Regional and Residual maps.

The difference between the regional map and the RTP map is observed in the absence of the local anomalies from the high and low anomalies in the first belt and the second belt within range from 42128 nT to 42331 nT. The second outcome is the residual map, which exhibits notable frequencies of high magnetic anomalies, restricted aerial extension, distinct amplitudes, and variable trends. These parameters reflect the variations in anomalies, sources, depths, compositions and structural settings. The residual range from -206 to 255 nT.

From Local wave number or (SPI), there are two magnetic sources, based on the depths to the magnetic sources: the shallow source and the deeper source based on the SPI results. With different sizes and trends, the magnetic source is located between 200 and 1400 meters below the surface (Crests and basins).

Generally, it could be summarized in (Spi) technique that the large low magnetic anomalies are linked with the deep basement while the large high anomalies are related to shallow basement.

The borders between high and low magnetic field data are identified using the horizontal derivatives method. The major and prominent fault direction is NW–SE, as revealed by the application of the (TDR) and (AS) techniques. In addition, the vertical derivative map's structural pattern indicates that the west of the section is identified by vast North W–South E and inverse N East–S West trend patterns. Likewise, the North and East parts in the region are similarly characterized by the NW-SE orientations.

The directions (trends) of the gradients and anomalies of RTP, regional, and residual magnetic trends (maps), as well as the trend analysis outcomes generated by using the rose diagram technique. The lineaments that was been identified on the maps indicate possible faults and/or contacts of different rock types with varying lengths and directions. This research area is influenced by numerous major trends NW-SE, NE-SW, E-W, NNE-SSW and WNW-ESE. In this regard, other minor structural patterns that appear on the rose diagrams are not notable, are shown in **(Fig. 10 (a), (b), (c), (d), (e), (f)) and Fig. 9(b)**.

Four 2D models are used in the construction of the basement structural cross-sections. These profiles are applied on RTP map. Determining the internal features that govern the presence and depth of valleys in the research area is the primary objective of these models. Further to assess the (bs) depth as well. The importance of valleys within the area, which may serve as radioactive element traps related to the geological setting.

8. Conclusions

The importance of valleys within the area, which may serve as radioactive element traps related to the geological setting. In the East parts and northwest regions in the study area, the basement surface descends to less than 170 meters, whereas in the southern region, it exceeds 1400 meters.

The depth of wadi Fatirah El-Beidah is within 230m, where it located at the intersection point between P2 and P3 at the northwestern part.

Wadi Abu Zawal extends from West to East in the north parts of the research area. It`s depth ranges vary from 700 m at the east, 400 m at the intersection point between P2 and P4 and to 170 m towards west.

Wadi Abu Shihat 1 and Wadi Abu Shihat 2 are located at the southwestern part and at the intersection point between p1 and P3. The depth of this wadi is within 1400m.

Wadi El Markh is in the southeastern part of research area. It`s depth varies from 700m at the south to 100 at the middle and 400 towards the northeast.

Ethics approval and consent to participate: This article does not contain any studies with human participants or animals performed by any of the authors.

Consent for publication: All authors declare their consent for publication.

Funding: Authors would like to thank Egyptian General Petroleum Corporation (EGPC) and Egyptian Geological Survey and Mining Authority (EGMA) and the Aero-Service Division of the Western Geophysical Company of America, USA for providing the data.

Conflicts of Interest: The author declares no conflict of interest.

Contribution of Authors: All authors contributed to the study, shared in reading, revising the Ms and approved the final manuscript.

Acknowledgement: The authors would like to great thanks for all help, efforts and supported by Egyptian General Petroleum Corporation (EGPC) and Egyptian Geological Survey and Mining Authority (EGMA) and Menofia University.

9. References

Abdel Ghani, I. M. (2001). Geology, petrology, and radioactivity of Gabal El-Urf area, Central Eastern Desert, Egypt (Ph.D. thesis). South Valley University, Sohag Branch, Egypt.

Aero-Service. (1984). Final operational report of airborne magnetic/radiation survey in the Eastern Desert, Egypt.Prepared for the Egyptian General Petroleum Corporation (EGPC) and the Egyptian Geological Survey and Mining Authority (EGSMA).

Ammar, A. A., El-Sadek, M. A., & Sabri, A. M. (1999). Utilization of aeroradiospectrometric survey data in defining radioelement anomalous zones in Elgalala Elbahariya-Elgalala Elqibliya area, Northern Eastern Desert, Egypt. In The First International Conference on the Geology of Africa, Assiut, Egypt (Vol. 2, pp. 315-339).

Asran, A. M., El-Mansi, M. M., Ibrahim, M. E., & Abdel Ghani, I. M. (2013). Pegmatites of Gabal El-Urf, Central Eastern Desert, Egypt. In The 7th International Conference on Geology of Africa, Assiut University, Egypt (Vol. 4, pp. IV.1-IV.22).

Baranov, V., & Naudy, H. (1964). Numerical calculation of the formula of reduction to the magnetic pole. Geophysics, 29(1), 67-79.

Baranov, V. (1957). A new method for interpretation of aeromagnetic maps: Pseudo-gravimetric anomalies. Geophysics, 22(2), 359-382.

Baranov, W. (1975). Potential fields and their transformation in applied geophysics. Gebrüder Borntraeger.

Bhattacharyya, B. K. (1965). Two-dimensional harmonic analysis as a tool for magnetic interpretation. Geophysics, 30(5), 829-857.

Bhattacharyya, B. K. (1967). Some general properties of potential fields in space and frequency domain: A review. Geoexploration, 5(3), 127-143.

Blakely, R. J., & Simpson, R. W. (1986). Approximating edges of source bodies from magnetic or gravity anomalies. Geophysics, 51(7), 1494-1498.

Boyd, D. (1969). The contribution of airborne magnetic surveys to geological mapping. In Mining and Ground Water Geophysics (pp. 213–227). Geological Survey of Canada, Economic Geology Report No. 26.

Conoco, C. (1987). Geological map of Egypt, scale 1: 500,000-NF 36 NE-Bernice, Egypt. The Egyptian General Petroleum Corporation, Cairo.

Debeglia, N., Martelet, G., Perrin, J., Truffert, C., Ledru, P., & Tourliere, B. (2006). Semi-automated structural analysis of high-resolution magnetic and gamma-ray spectrometry airborne surveys. Journal of Applied Geophysics, 58(1), 13-28.

El-Mansi, M. M., & Dardier, A. M. (2005). Contribution to the geology and radioactivity of the older granitoids and younger granites of Gabal El-Urf-Gabal Abu Shihat area, Eastern Desert, Egypt. Delta Journal of Science, 29(2), 1-17.

El-Tahir, M. A. (1978). Relation between geology and radioactivity of some basement rocks to the north of Qena-Safaga asphaltic road, Eastern Desert, Egypt (Master's thesis). Faculty of Science, Al-Azhar University, Cairo.

El-Leil, I. A., Bekhit, M. H., Tolba, A. S., Moharem, A. F., & Shahin, T. M. (2015). Geological, structural and petrotectonical aspectable features of Neoproterozoic rocks, Gabal El Dob area, Northeastern Desert, Egypt. International Journal of Scientific Engineering and Applied Science, 1(8), 332-350.

Garcia, J. G., & Ness, G. E. (1994). Inversion of the power spectrum from magnetic anomalies. Geophysics, 59(3), 391-401.

Geosoft Inc. (2015). Data processing and analysis systems of Earth science applications (Ver. 8.3.3). Geosoft Inc., Toronto, Canada.

Grauch, V. J. S., & Johnston, C. S. (2002). Gradient window method: A simple way to separate regional from local horizontal gradients in gridded potential-field data. In SEG International Exposition and Annual Meeting (pp. 762–765). SEG.

Hamimi, Z., Hagag, W., Fritz, H., Baggazi, H., & Kamh, S. (2022). The tectonic map and structural provinces of the late Neoproterozoic Egyptian Nubian Shield: Implications for crustal growth of the Arabian-Nubian Shield (East African Orogen). Frontiers in Earth Science,10,921521. https://doi.org/10.3389/feart.2022.921521

Hamimi, Z., Eldosouky, A., Hagag, W., & Kamh, S. (2023). Large-scale geological structures of the Egyptian Nubian Shield.ScientificReports,13(1923). https://doi.org/10.1038/s41598-023-29008-x

Kusky, T. M., Abdel Salam, M. G., Stern, R. J., & Tucker, R. D. (2003). Evolution of the East African and related

orogens, and the assembly of Gondwana. Precambrian Research, 123, 81-338.

Lghoul, M., Abd-Elhamid, H. F., Zeleňáková, M., Abdelrahman, K., Fnais, M. S., & Sbihi, K. (2023). Application of enhanced methods of gravity data analysis for mapping the subsurface structure of the Bahira basin in Morocco. Frontiers in Earth Science, 11, 1225714.

Maurizio, F., Tatina, Q., & Angelo, S. (1998). Exploration of a lignite-bearing formation in Northern Ireland, using ground magnetic surveys. Geophysics, 62(4), 1143-1150.

Phillips, J. D. (2000). Locating magnetic contacts: A comparison of the horizontal gradient, analytic signal, and local wavenumber methods. In SEG Technical Program Expanded Abstracts 2000 (pp. 402-405). Society of Exploration Geophysicists.

Spector, A., & Grant, F. S. (1970). Statistical models for interpreting aeromagnetic data. Geophysics, 35(2), 293-302.

Stern, R. J. (1994). Neoproterozoic (900-550 Ma) arc assembly and continental collision in the East Africa orogen: Implications for the consolidation of Gondwanaland. Annual Review of Earth and Planetary Sciences, 22, 319-351.

Thurston, J. B., & Smith, R. S. (1997). Automatic conversion of magnetic data to depth, dip, and susceptibility contrast using the SPI™ method. Geophysics, 62(3), 807-813.

Verduzco, B., Fairhead, J. D., Green, C. M., & MacKenzie, C. (2004). New insights into magnetic derivatives for structural mapping. The Leading Edge, 23(2), 116-119.

Wijns, C., Perez, C., & Kowalczyk, P. (2005). Theta map: Edge detection in magnetic data. Geophysics, 70(4), L39-L43.

تطبيق التقنيات المحسنة لبيانات المغناطيسية الجوية لدراسة التركيب تحت السطحي في منطقة العرف، الصحراء الشرقية الشمالية، مصر

نها محمد حسن[١]، ومصطفي عبدالوهاب زعيمة[٢]، ومحمد فاروق أبوحشيش[١]، ومنارمحمد البرم[١]

[١] قسم الجيولوجيا، كلية العلوم، جامعة المنوفية، مصر

[٢] هيئة المواد النووية، ص.ب ٥٣٠، المعادي، القاهرة، مصر

تم الحصول على بيانات المغناطيسية الجوية من قبل شركة أيرو- سيرفيس (Aero-Service) في عام ١٩٨٤ في الصحراء الشرقية بمصر،وتشمل منطقة جبل العرف وما حولها. تتكون صخور القاعدة ما قبل الكمبري (Precambrian) بشكل رئيس على الجرانيتات الحديثة (Gy) .علاوة على ذلك، قد تحتوي منطقة الدراسة على مواد مشعة. تشير القياسات المغناطيسية إلى تباينات في أعماق المصادر والقابلية المغناطيسية. لذلك، تُستخدم هذه البيانات لتحديد أماكن وأعماق الأجسام المغناطيسية. يتناول هذا العمل فصل خريطة الأختزال إلي الأقطاب (RTP) للكشف عن المصادر االعميقة والمصادر السطحية من خلال استخدام طيف القدرة(Power Spectrum). تبين من استخدام الفصل أن صخور القاعدة تتواجد في أعماق تتراوح بين ٢٠٠ متر إلى أكثر من ١٥٠٠ متر وأقل من ٢٠٠ متر للضوضاء. من خلال استخدام تقنية صور معامل المصدر(SPI)، تُظهر هذه الطريقة نتائج مماثلة. تقع مصادر صخور القاعدة بين ١٥٠ إلي حوالي ١٥٠٠ متر تحت السطح. تم تحديد الأتجاهات لمنطقة الدراسة والفوالق السطحية والفوالق التحت سحية من خلال تفسير البيانات المغناطيسية. الاتجاه الرئيسي للفوالق في خريطة الأختزال إلي الأقطاب من مخطط الوردة(Rose Diagram) في منطقة الدراسة هو شمال شرق - جنوب غرب. هناك أيضًا اتجاه آخر من شمال غرب - جنوب شرق شرق - غرب. بالنسبة للخريطة الإقليمية (Regional)، فإن الاتجاه الرئيس لمنطقة الدراسة هو شمال شمال شرق - جنوب جنوب غرب . بالإضافة إلى ذلك، هناك اتجاه آخر من شمال غرب - جنوب شرق شمال شرق - جنوب غرب. بالنسبة لخريطة المتبقي (Residual) ، فإن الاتجاهات الرئيسية في منطقة العمل هي شمال غرب - جنوب شرق، شمال شرق - جنوب غرب، غرب شمال غرب - شرق جنوب شرق و شرق - غرب. يتبين من الدراسة الفوالق المقترحة على طول بروفيلين من الغرب إلى الشرق و بروفيلين عموديين من الجنوب إلى الشمال، ويحدد قيم العمق لنقطة تقاطعها. إن عمق الوديان في منطقة البحث هو النتيجة النهائية والأكثر أهمية فيما يتعلق بهدف الدراسة. هذا لأن المواد المشعة يُعتقد أنها متمركزه بها.